GeoJournal 17.4 597–613

On the Geoecology of Southern Tibet*

Measurements of Climate Parameters Including Surface- and Soil-Temperatures in Debris, Rock, Snow, Firn, and Ice during the South Tibet- and Mt. Everest Expedition in 1984

Kuhle, Matthias, Prof., Dr.; Jacobsen, Jens-Peter, Dipl.-Geogr.,
Universität Göttingen, Geographisches Institut,
Goldschmidtstraße 5, 3400 Göttingen, FR Germany

Radiation and Radiation Balance

Between 8 September and 23 October 1984 incoming radiation (0.3–3.0 μm) was measured with a Thies actinograph at heights between 5000 m and 6500 m at six stations for a total of 30 days (Fig 1). These were as follows:

1) Shisha Pangma Base Camp 28° 36'N 85° 45'E 5000 m 4 days
2) Shisha Pangma Camp I 5300 m 1.5 days
3) Shisha Pangma Camp II on the Yepokangara glacier (Fig 2) at 5540 m 1.5 days
4) Central Rongbuk glacier (orographic right paraglacial valley on Mt. Everest N slope) 28° 05'N 86° 52'E at 5500 m (Camp I) 10 days
5) East Rongbuk glacier medial moraine (Mt. Everest N slope) 6040 m (Camp II) almost 5 days
6) East Rongbuk glacier (Camp III) at 6500 m 7.5 days

On 21 September (the beginning of autumn) a theoretical value of global radiation of 1180 W/m^2 is possible at these heights in this region, ignoring the transmission absorption of the atmosphere. Since this date lies halfway through the expedition this may be taken as a mean for this value during the expedition. Fig 1 gives the decrease of global radiation during the period and shows that with values over 1200 W/m^2 these theoretical values for the upper limit of the atmosphere were reached at comparable solar altitudes. This shows the extreme transparency of the atmosphere above 5000 m.

Simultaneous observations of such high global radiation values were made on a Dirmhirn Starpyranometer (0.3–3.0 μm; measurement period 9 September to 3 November 1984), Lambrecht radiation-balance meter (0.3–60 μm; same period) and a Thies radiation-balance meter (0.3–60 μm; 10 October to 20 October 1984) (Fig 3). The values above 1200 W/m^2 are the result of reflection from the lower surfaces of small amounts of cloud (2/8) and from ice pyramids (Fig 2) (Fig 3 middle row: East Rongbuk glacier at 6040 m).

Fig 3 also shows the way the albedo depends on the surface. For comparable incident radiation values this reaches 180–290 W/m^2 with sporadic patches of mat vegetation, almost 500 W/m^2 from bright quartz sand and over more than 600 W/m^2 between ice pyramids (Fig 2). Reflected energy reaches even higher levels from bare firn. In the area of the glacier catchment the snow surface at 6650 m reflected more than 850 W/m^2 from an incoming radiation of less than 1000 W/m^2 (Fig 4 and 5, foreground). Fig 6 presents the albedo values (per cent) of specific materials from the Mt. Everest region. The albedo from dark debris amounted to about 14–16%, so that in comparison to the fresh snow cover the difference in albedo reaches 80% at the most. Generally, a difference of about 70% was measured between unglaciated surfaces and glacier catchments.

The low albedo values of the debris can be seen in its high soil temperatures measured at the same time; e.g. at Shisha Pangma at 5540 m where the soil temperatures at 1 cm in gravel reached 20° C (Fig 13). Fig 14 shows such a value of about 30° C measured on Mt. Everest at

* Paper discussed at the International Tibet-Symposium at Göttingen, October 8–11, 1985

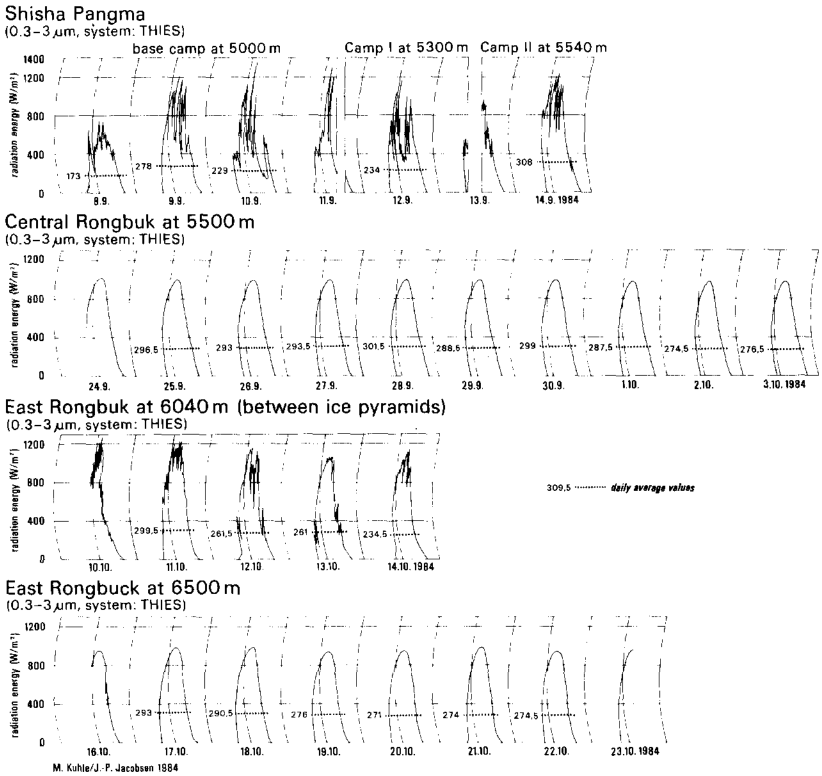

Fig 1
Global radiation in S Tibet and on the N slope of the Himalaya (Shisha Pangma, Mt. Everest) between 28°N and 28°35'N

Fig 2 Ice pyramids of the glacier tongue of the Yepokangara glacier at 5600 m (28°25'N 85°46'E). The retreating glacier tongue is disintegrating into these c. 30 m high ice pyramids (scale provided by figure of man). Such glaciomorphological forms are characteristic of the subtropical radiation energy conditions in S Tibet in the precipitation shadow of the High Himalayas and are much more strongly developed than on the leeside S slope of the Himalayas. Photo: M. Kuhle, 13 September 1984

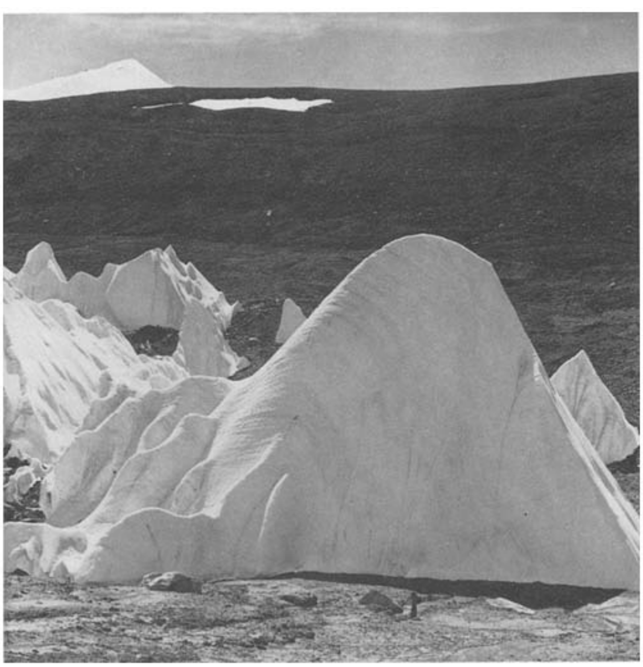

1.25 pm on a cloud-free autumn day. No doubt, soil temperatures expecially in small depth depend on both incident radiation (cloud cover) and wind velocity (Fig 7–11).

Cloud Cover, Wind Direction and Velocity, Relative Humidity, Air Temperature, and Soil Temperatures at 1 cm, 5 cm and 10 cm

Fig 7–11 show continuous fixed measurements at the following locations and dates: Fig 7 Shisha Pangma Base Camp (5020 m, 28°36'N 85°45'E) 7 to 16 September; Fig 8–11 Mt. Everest Base Camp (5170 m, 28°11'N 86°51'E) from 8 to 11 September and on Himalaya N slope from 17 September to 4 November 1984.

These illustrations show the daily freeze-thaw alternations up to 10 cm deep in a representative year as the monsoon season changes to clear, cold and stormy autumn days. Moisture first enters the surface material; then follow the solifluction movements of debris of 4 to 8 cm/year measured by this expedition on slopes of 30° on scree-cones, debris slopes and morainic slopes.

Fig 12 to 17 present the observations and measurements obtained by portable instruments. The values from Shisha Pangma at 5300–5640 m and those from Rongbuk glacier on Mt. Everest were obtained at the same time as those on Fig 7–11. These provide for a comparative interpretation and the determination of rates of altitudinal change (lapse rates). Values repre-

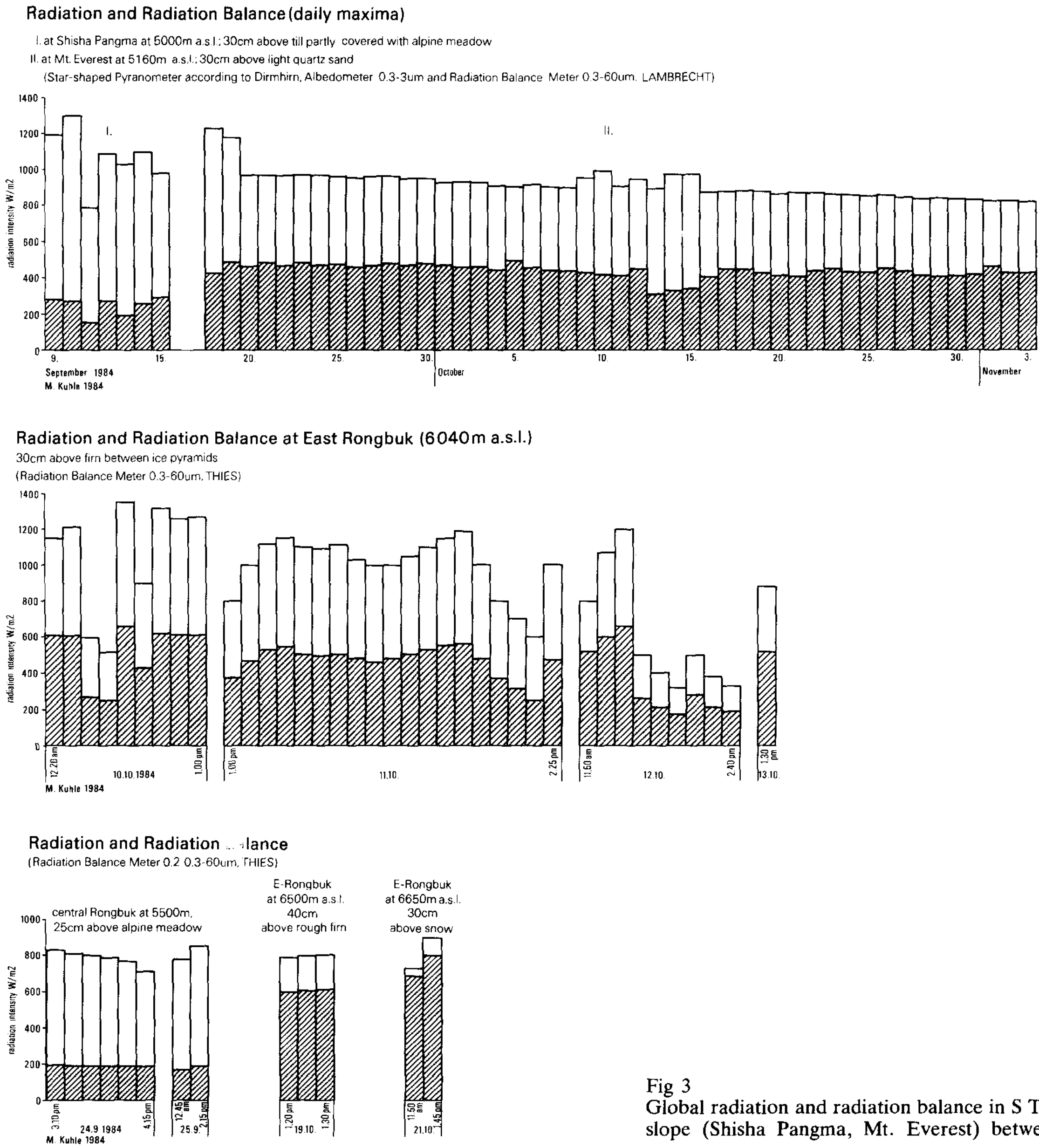

Fig 3
Global radiation and radiation balance in S Tibet on the Himalaya N slope (Shisha Pangma, Mt. Everest) between 28°N and 28°35'N

sentative of the S Tibetan area and the Tibetan Himalaya in the lee of the High Himalayas are provided by the measurements at Latsu (29°N 87°40'E) between 4030 m and 5000 m and at Nilamu (28°11'N 85°58'E) at 4300 m from 25 August until 7 September.

The following characteristic tendencies are recognizable:

a) Cloud cover decreases from 8/8 to 0/8.
b) From mid-September the wind direction ceases to vary and becomes stable from a prevailing SSE to SE point.
c) In the areas near the valley floors the wind velocity, which reached only a few metres per second reached up to 20 m/sec in the autumnal post-monsoon period. The up to 100 m long snow banners streaming from the peaks which were observed from the beginning of October became very much longer, clearly influenced by the jet-stream velocities which probably reached 30 or even 40 m/sec. These cleared the rock surfaces above 7200 m of snow and were effective in forming the upper limit of glaciation (see below).
d) The relative humidity (and since temperature decreases also occurred, the absolute humidity) decreased from 60–90% in the monsoon period to 10–20% in the autumnal post-monsoon period. At the same time sudden excursions of humidity to 80 or 90% or more became steadily less regular and frequent (Fig 7–11). These suddenly increased humidity periods were associated with veering of wind from SE to W, NW and N and its simultaneous decrease in velocity; during them cloud cover increased from 0/8 to 1/8 and as much as 5/8.

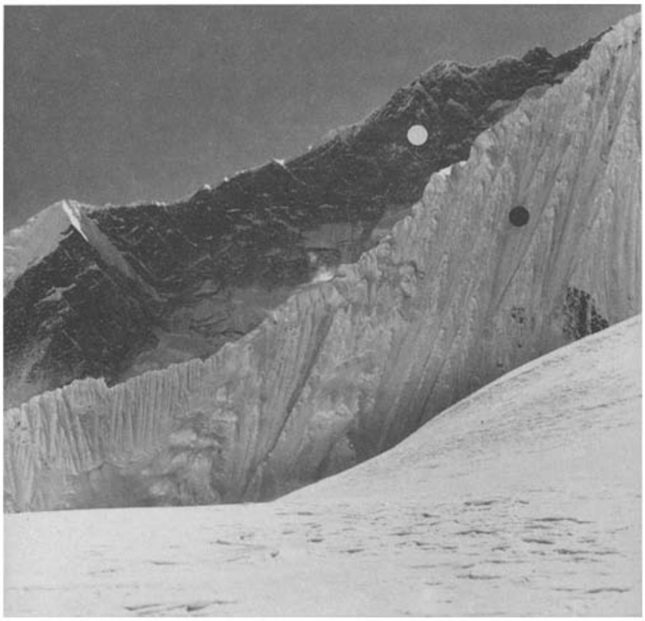

Fig 4 View of Lhotse, 8501 m (27°58'N 87°00'E), from the N (● white) from Rapiu La (6500 m). Although the E spur (● black) of Mt. Everest is of similar steepness and is covered with cornices and ice wall some decametres thick, the metamorphite of the Lhotse wall (● white) reaching over 7200 m is unglaciated and is blown almost free of snow (cf. Fig 5). Photo: M. Kuhle, 19 October 1984

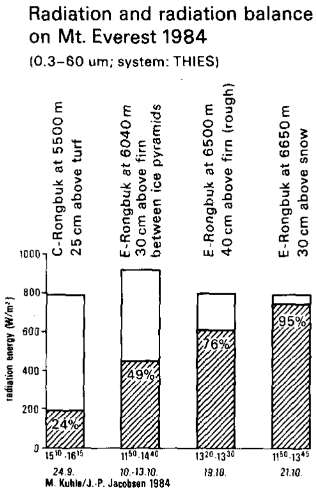

Fig 6
Radiation and radiation balance on Mt. Everest 1984

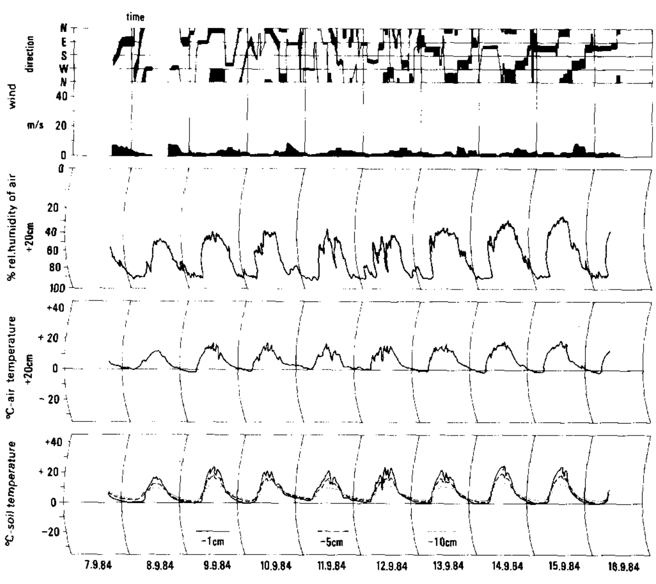

Fig 7 Measurements at the fixed base camp on Shisha Pangma N slope (28°35'N 85°46'E) at 5020 m on moraine debris with mat vegetation

Fig 5 View of Makalu, 8481 m (27°54'N 87°05'E), from the NNW from Rapiu La (6500 m). On this mountain, formed of massive tourmaline-granite in contrast to the metamorphic rocks of Mt. Everest, a clear upper glacial limit (——) can be seen. It runs between 7200 m and 7600 m on its W wall (●). The NE flank of the mountain lies in wind shadow and thus carries a hanging glacier in a cirque-like feature (×) at above 7600 m.
Photo: M. Kuhle, 19 Oct. 1984

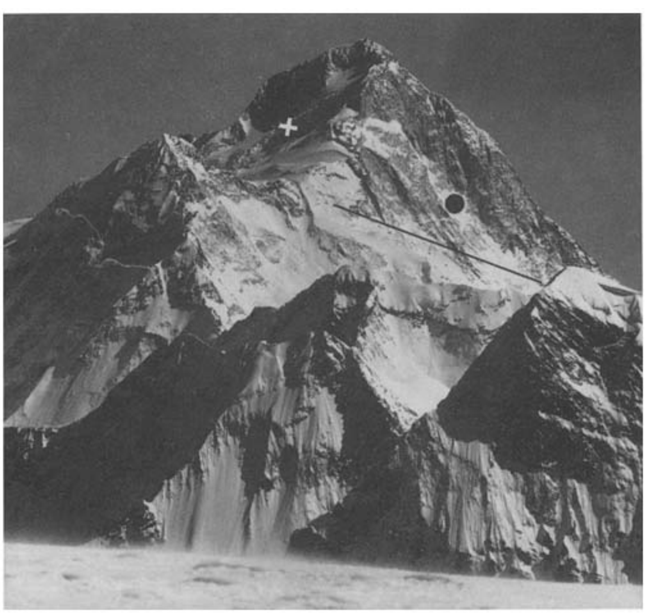

e) Air temperature decreased as the solar altitude showed its seasonal decrease. On the debris surfaces of the valley floors and high plains at 5000 m these reached almost 20° C at midday and fell to only a few degrees below freezing at night. In October and November this same diurnal variation (about 20° C) is 10° C to 15° C lower down the scale. The maximum daily heating occurred on the upper moraine at 6500 m at 11,45 hr on 19 October when the air temperature at 2 m over the surface reached +7° C and at 2 cm above the ground +27° C. It is interesting that air temperatures were independent of the humidity increases referred to above. In each case there was no reduction in cooling at night during high humidities; it was rather slightly increased (Fig 9: 3–6 Oct.; Fig 11: 29 and 30 Oct).

Fig 8–11
Measurements at the fixed Mt. Everest base camp in the Rongbuk valley (Himalaya N slope) on the tongue of the Rongbuk glacier at 5170 m (28°10'N 86°51'E) from 17 September to 4 November 1984

Fig 8

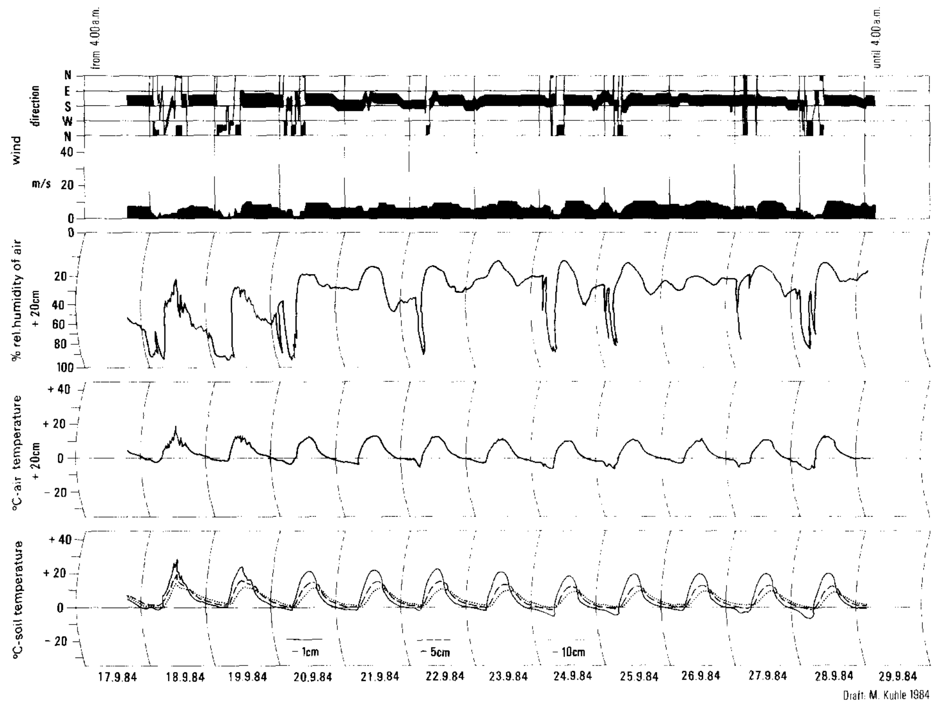

Fig 9

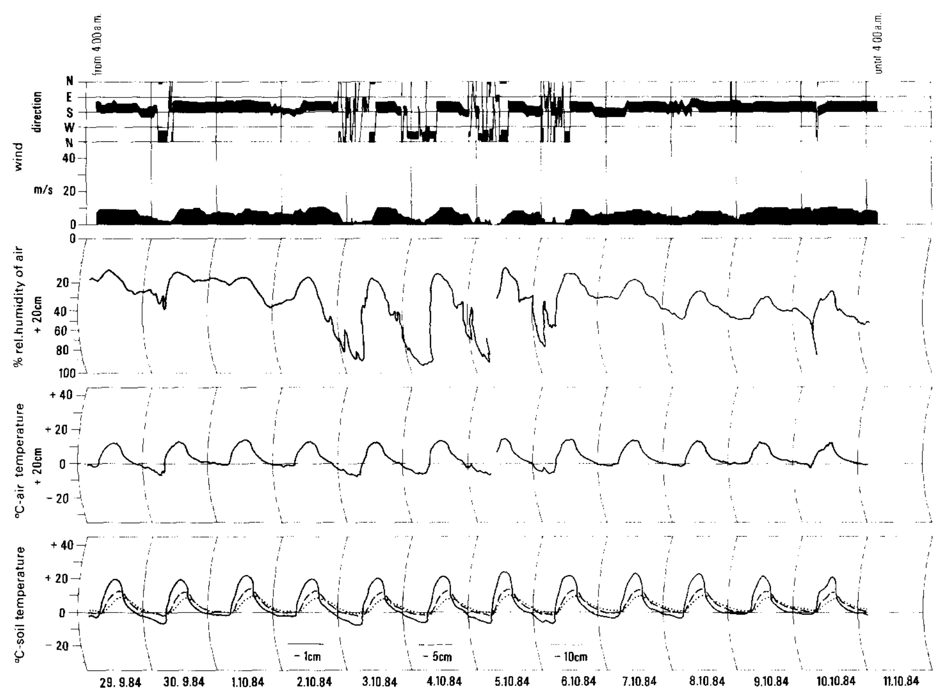

f) The diurnal variation of soil temperature, which follows the air temperature, is reduced as depth of observation increases from –1 cm to –10 cm. Periglacially active freezing in the debris began on 20 September at –1 cm and on 29 September at –10 cm (Fig 8). On the other hand the soil above –10 cm no longer thawed after the beginning of November. Thus the periglacially active freeze-thaw layer traversed the upper 10 cm of soil in 45 days (cf. Kuhle 1985). This produces a new picture of the relatively short seasonal transition period of periglacial processes in subtropical S Tibet at 5000 m. Not only is the period of periglacial soil movement here shorter than in temperate latitudes but, since the ground ceases to thaw down to 10 cm after a short time, it is also restricted in depth.

The columns for Latsu (Fig 12) and Nilamu (Fig 13) make clear the relation between inversions of temperature and increasing attenuation of energy flux with depth. Thus at 05,15 hr on 26 August with 15° C at

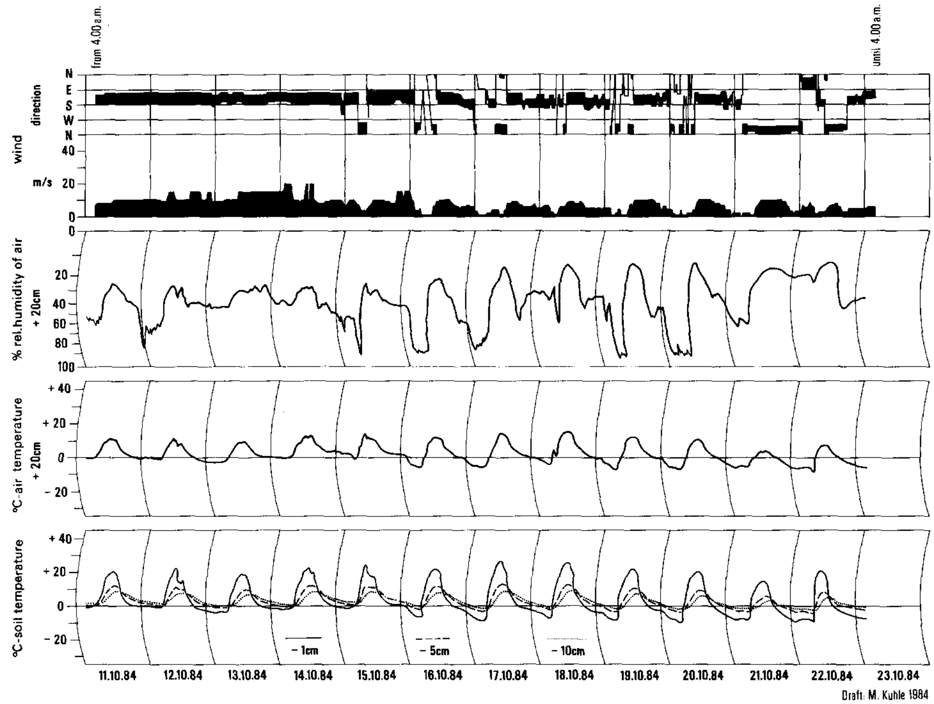

Fig 10

Fig 11

−10 cm but 12° C at −1 cm at 12,00 hr (am) in contrast it was only 13.5° C at −10 cm but 15.5° C at −1 cm.

g) All the sinusoidal diurnal curves of air and soil temperature as well as relative and absolute air dryness (inverse humidity) are related in the same sense to the curve of air temperature. Soil temperatures show a lag because of its insulating effect on the flux of energy. Wind velocity varies independently of wind direction and in this area is independent of time of day.

h) The mean air temperature of −9° C to −11° C at the snowline (ELA) extrapolated from the values of Fig 7 to 17 shows that the S Tibetan glaciers of the N slope of the Himalaya and the Tibetan glaciers are cold-arid ice-flows. They are correctly contrasted by Shi Yafeng and Xie Zichu (1964) as continental rather than belonging to the more maritime monsoon influenced glaciers of obviously warmer regions.

Fig 12
Measurements with hand transportable equipment in the Tibetan Himalaya S of the Tsangpo depression (29°03'N 87°42'E)

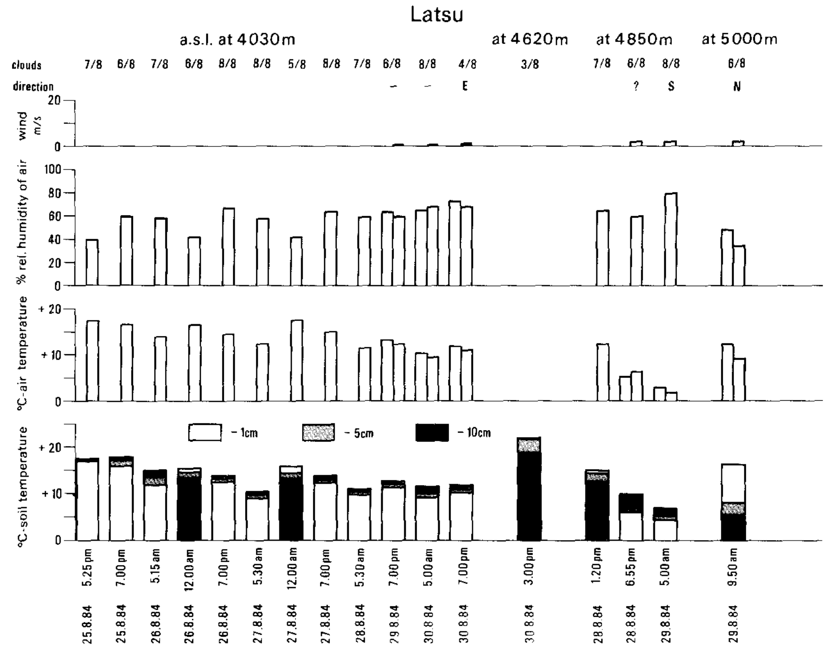

Fig 13
Measurements with hand transportable equipment in the Tibetan Himalaya and on the N slope of the High Himalaya (28°12' to 40'N 85°40' to 86°10'E)

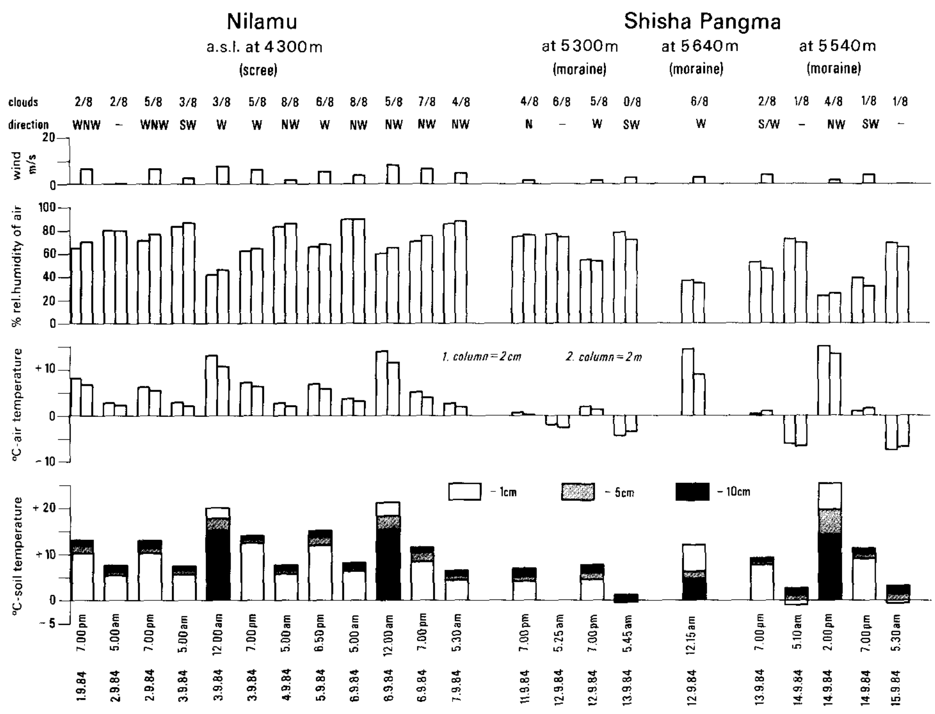

Surface Temperatures on Mountain Slopes between 3800m and 8800m on Debris, Rock, Ice, Firn, and Snow

In the post-monsoon periods of 1982 and 1984 at times between 18 September and 4 November measurements were made in the High Himalayas of the surface temperatures with all exposures; in more detail this was on the N and S slopes of the Mt. Everest group. These concentrated on collecting data during cloud free radiation weather situations because of the telemetric measurement methods using passive infra-red detectors (Kuhle 1986a and 1986b). As the humidity measurements for the same periods show (Fig 8–11, 14–17) the air water content was then very small. This was not only because of the low temperatures measured at the same time as the specific humidities but also because of the low atmospheric density above 3800 m. Because of this transparency of the atmosphere to the transmission of energy (infra-red radiation between 8 and 14 μm) is almost complete so that there is almost no selective absorption

Fig 14

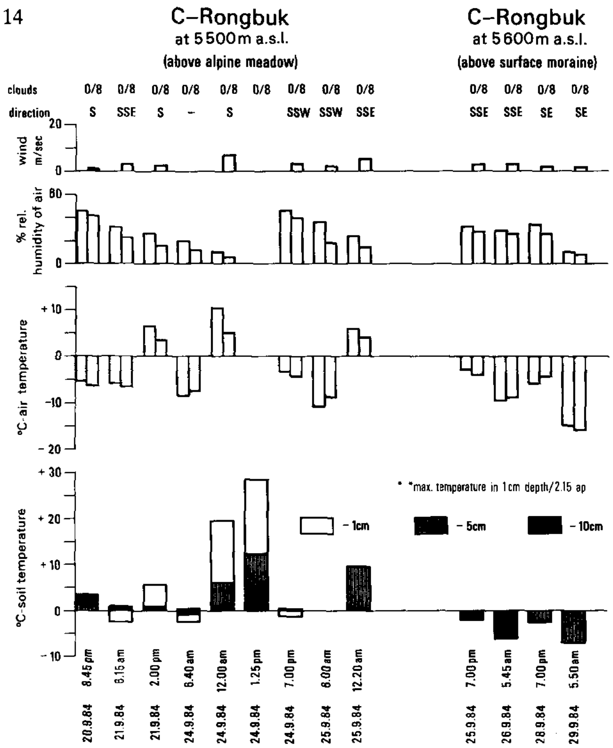

Fig 15

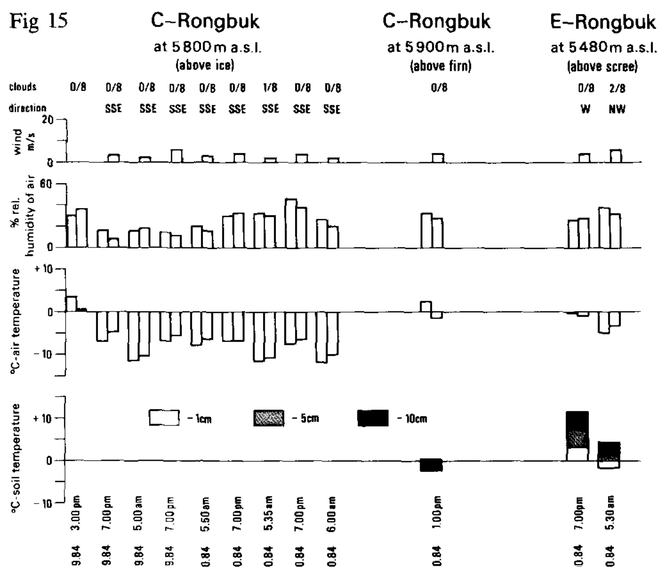

Fig 16

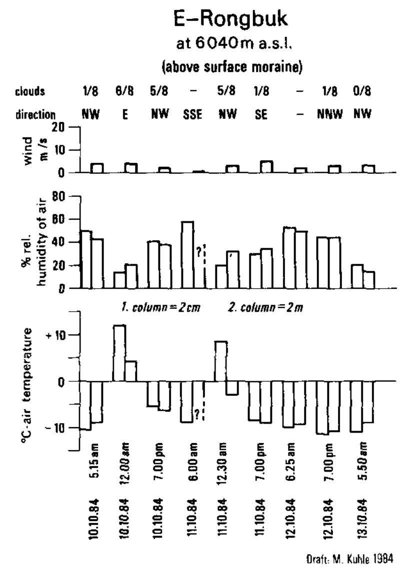

Fig 17

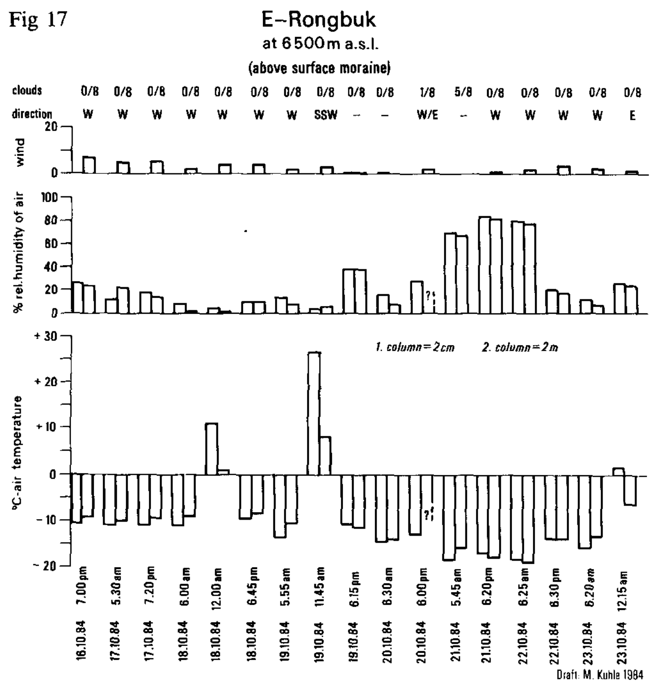

Fig 14–17 Hand portable and fixed measurements near and on the glaciers of the Mt. Everest N slope (Central and East Rongbuk glaciers between 5480 m and 6500 m, 28° to 28°08'N 86°50' to 58'E) from 20 September to 23 October 1984

by the air and thus the measured values represent the true surface temperatures.

Since the measurement techniques are described in previous works (Lorenz 1973; Kuhle 1986 a+b) they are referred to only briefly. We used instruments with 100 m focal length concave mirrors and distances of 1500, 3000 and 6000 m. These were types R 380 RVC (Raynger, USA), Thermopoint 80 (AGA, FRG) and Raynger II HR (Raynger, USA). They are specially adepted for extremely low temperatures. The concave mirrors focus the radiation on an electronic chopper and process the infra-red portions. Although the miniature R 380 RVC instrument required calibration over a black plate both the digital instruments were provided with corrections for specific conditions. The microprocessor controlled instruments are provided with telescopic sights and are accurate to ±1%. For calibration some of the surface temperatures were compared with resistance thermometer measurements on the same objects.

The results obtained are presented in Fig 19–29 and summarized in the table forming Fig 30. For statistical reasons the temperature gradients were not separated according to slope exposure so the rather inhomogeneous 1775 data points include all four or even eight compass directions. The regression analyses provided (Pearson product moment correlation) show R values correlation ranging from -0.82327 to -0.66111 with an overall value of $R = -0.78000$ with a propable error of less than 1% (significance -0.00000) so that meaningful conclusions can be drawn. These referred to both the temperature gradients per 100 m (A, B) and the position of the 0° C line on rock (Fig 19–21) and ice (Fig 22–24) surfaces between 11 hr and 15 hr local time (Fig 19, 22, 25) and between 15 hr and 11 hr (Fig 20, 23, 26). Fig 21 includes all values on rock surfaces and Fig 24 all such values on ice surfaces. Fig 25 and 26 include rock and ice substrates together, dividing the values between 11 hr and 15 hr from those between 15 hr and 11 hr. The curves of Fig 27 investigate all 1775 observations of surface temperatures of both surface types and time intervals.

Above and below the regression lines (the solid lines) of Fig 19 to 27 are shown by single (dashed) and double (dotted) standard errors of estimation (SEE). The former should include 66%, the latter 95%, of all possible surface temperatures. The height at which the double SEE line cuts the 0° C line is that for which there is a 95% probability that the temperature will not rise above freezing point. Similarly the intersection with the single SEE line shows the height at which melting rarely occurs on the slopes of the Himalayas. This is already at an altitude with a mean annual temperature of −25° C or less. At this height, above the 0° C limit, there can be no snow settling or sintering process such as occurs in warmer, near freezing point areas i.e. no ice bridges can form between new snow nuclei. Firn formation by a temperature induced metamorphosis is absent. The snow remains dry and cohesionless and does not cling to the rock. It is easily blown from the summit pyramids by the storms at this altitude. Thus there is formed a glacier-free rocky altitudinal zone above that of the glaciers as the highest tier of the climato-geomorphological vertical zonation of the Earth (Kuhle 1986a, b; 1987).

This upper limit of the glacial zone is clearly developed on Mt. Everest, Makalu and Lhotse in the central Himalayas at some 7200 m. At this height bare rock comes to the surface (Fig 4 -------, Fig 5, 28, 29 -------). This height of the empirical upper limit of glaciation makes sense in terms of Fig 19–21 and 25 and especially of the curves of the combined data in Fig 27. In all these graphs the height of 7200 m comes between the 0° C intersections of the double SEE lines. In the middle of this height zone between 6600 m and 7700 m (Fig 27) the cold, cohesionless snow is almost completely blown away like dry wind-blown sand. This average height of the upper limit of glaciation varies with the exposure of the

Fig 18 View from 6340 m over the East Rongbuk glacier (in shadow in foreground) towards the NE to its confluence with the Khartaphu glacier (28°02' to 30'N 86°59'E). The cross-sections of both the Khartaphu glacier (▽) and that of the tributary cirque glacier (●) are both box-like, i.e. with almost vertical steep edges (▼). This denotes a cold arid glacier flow mechanism (block flow movement). Such profiles occur at the snow line where mean annual temperatures of −9° C to −10° C are found. This is also the mean temperature of the glacier at about 10 m in the ice and indicates a cold continental type of glacier.
Photo: M. Kuhle, 17 October 1984

mountain slopes to sun and wind and also, though only slightly, with the steepness of the rock walls.

Fig 30 provides the relationship between the height of the 0° C level based on the time of day and nature of the surface and the thermal zonation (temperature gradient). On rock surfaces this varies 870 m between day (representing the insolation between 11 hr and 15 hr) and night (low radiation balance between 15 hr and 11 hr). It varies twice as much on ice (1681 m). This height limit has a mean value of 5719 m on rock but some 800 m lower, 4913 m, on ice. The differential effect of the surface material is seen by the steeper gradient on rock (Fig 19–21). The less steep increase on ice surfaces may be explained by the loss of sensible heat below the 0° C line resulting from melting (which requires latent heat (Fig 22–24). This also explains the much lower mean level of the 0° C boundary over ice. The diurnal difference lies between these two extremes on a composite rock/ice surface. The distribution shown gives this as 953 m; the difference in height of the 0° C line between rock and ice is 593 m between 11 hr and 15 hr, and 1404 m between 15 hr and 11 hr. This illustrates both the greater absorption of heat by the dark rock surface and its greater heat capacity above freezing

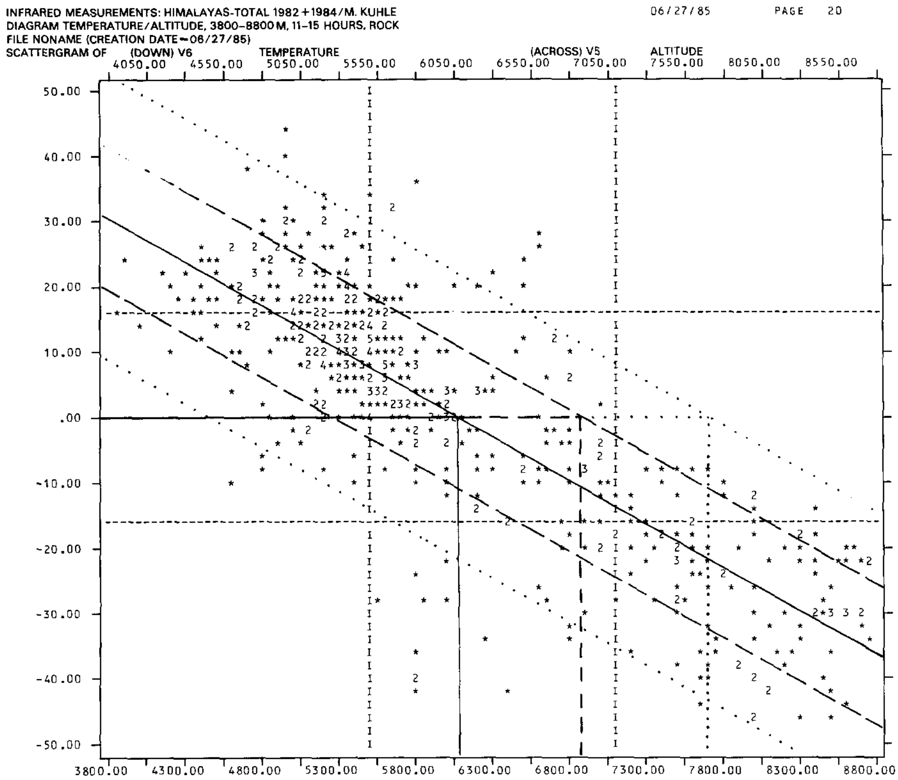

Fig 19

Fig 19–27
Telemetric infra-red measurements in the Mt. Everest massif (High Himalaya 27°57' to 28°10'N 86°45' to 87°E) on rock, debris, snow, firn and ice surfaces of valley glaciers, valley sides and the highest mountain slopes

STATISTICS..

CORRELATION (R)-	-.82327
STD ERR OF EST -	10.88582
PLOTTED VALUES -	554
R SQUARED -	.67778
INTERCEPT (A) -	82.13377
EXCLUDED VALUES-	5
SIGNIFICANCE -	.00000
SLOPE (B) -	-.01353
MISSING VALUES -	0

GRADIENT OF TEMPERATURE: 1.353°C/100 M

0°C-LINE AT 6070 M

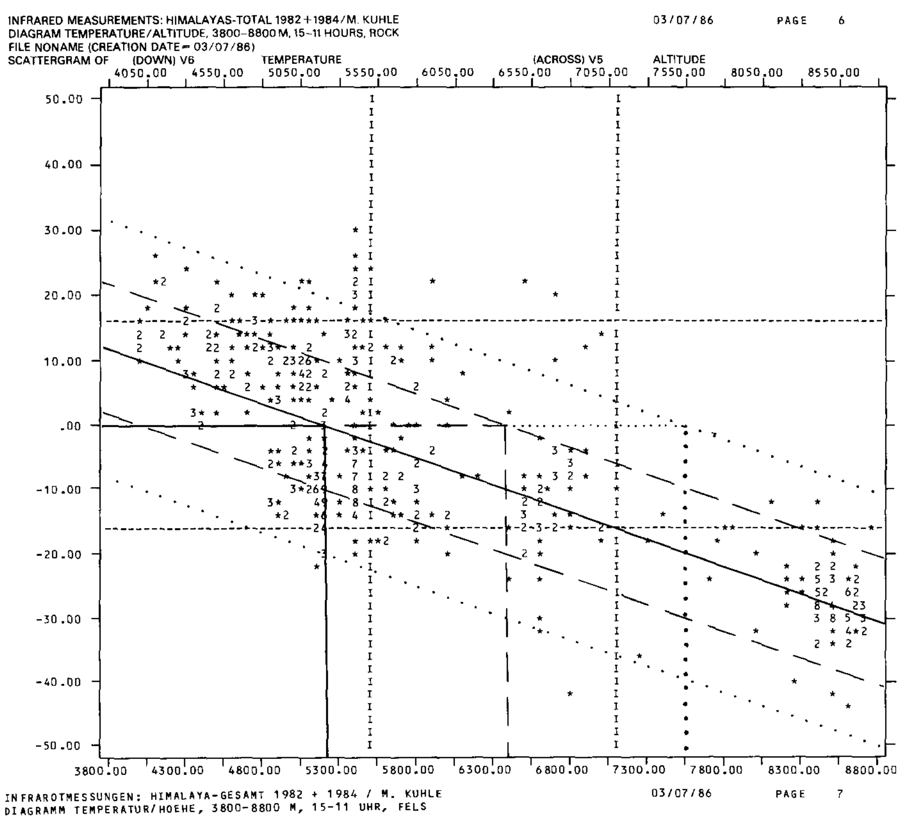

Fig 20

STATISTICS..

CORRELATION (R)-	-.7599
STD ERR OF EST -	9.97278
PLOTTED VALUES -	536
R SQUARED -	.57759
INTERCEPT (A) -	44.24800
EXCLUDED VALUES-	3
SIGNIFICANCE -	.00000
SLOPE (B) -	-.00851
MISSING VALUES -	0

GRADIENT OF TEMPERATURE: 0.851°C/100 M

0°C-LINE AT 5200 M

Fig 21

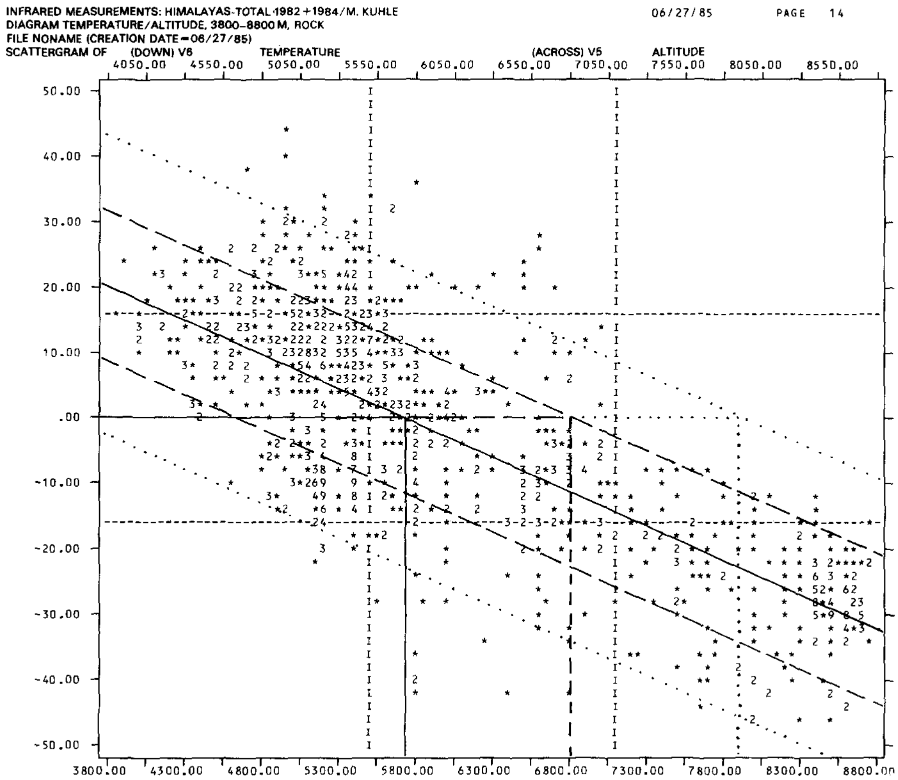

STATISTICS..

CORRELATION (R)-	-.75686
STD ERR OF EST -	11.57066
PLOTTED VALUES -	1090
R SQUARED -	.57284
INTERCEPT (A) -	60.27774
EXCLUDED VALUES-	8
SIGNIFICANCE -	.00000
SLOPE (B) -	-.01054
MISSING VALUES -	0

GRADIENT OF TEMPERATURE: 1.054°C/100 M

0°C-LINE AT 5719 M

Fig 22

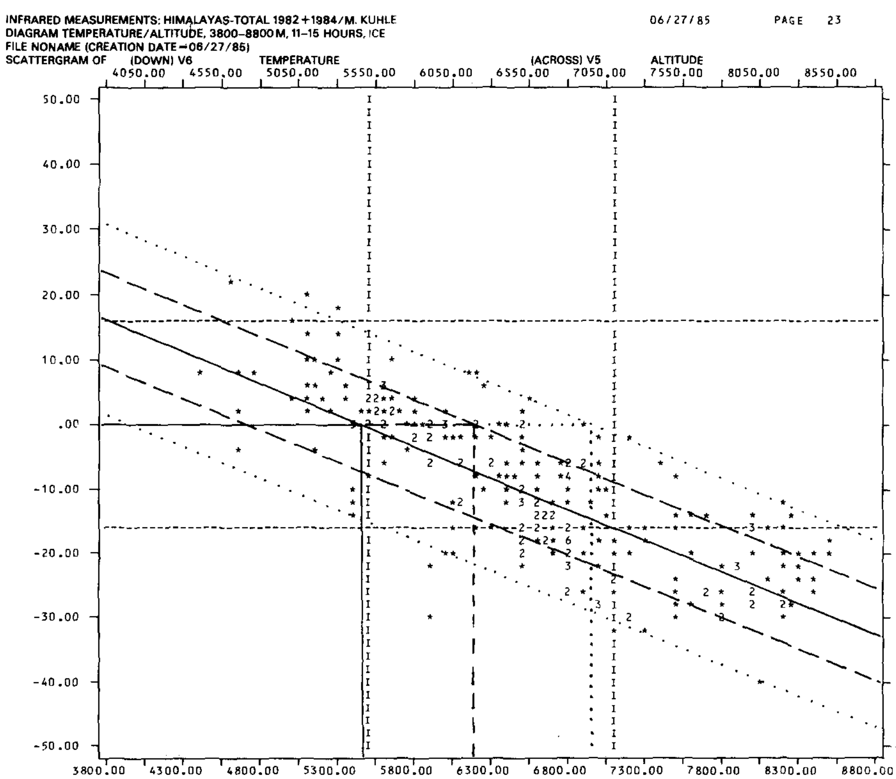

STATISTICS..

CORRELATION (R)-	-.78515
STD ERR OF EST -	7.31610
PLOTTED VALUES -	259
R SQUARED -	.61645
INTERCEPT (A) -	54.16874
EXCLUDED VALUES-	0
SIGNIFICANCE -	.00000
SLOPE (B) -	-.00989
MISSING VALUES -	0

GRADIENT OF TEMPERATURE: 0.989°C/100 M

0°C-LINE AT 5477 M

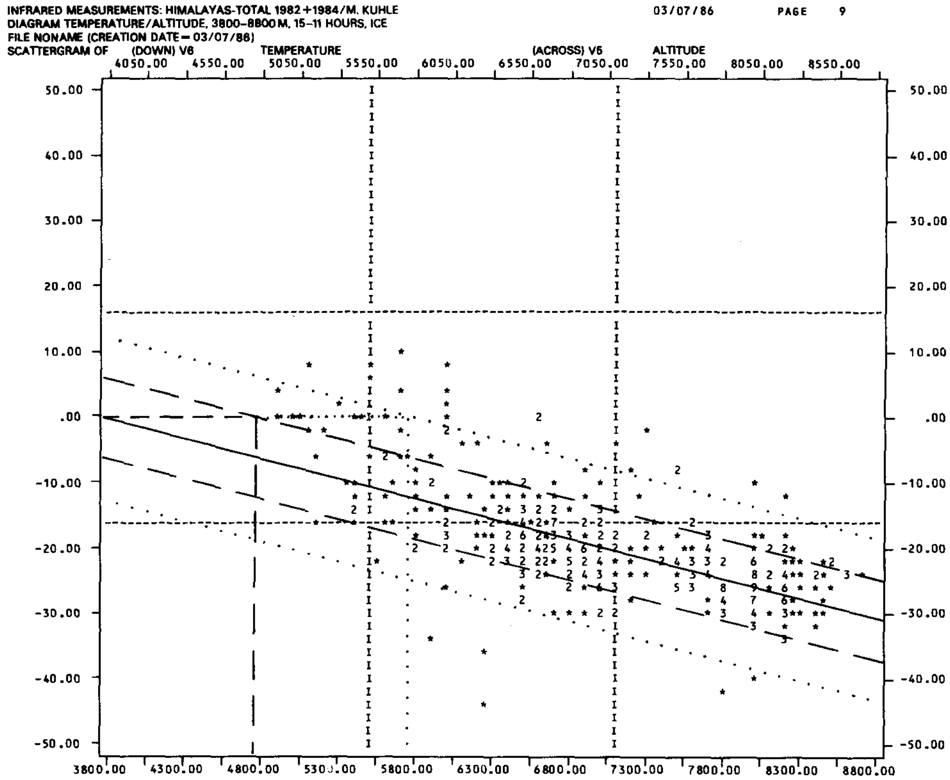

Fig 23

STATISTICS..

CORRELATION (R)-	-.66111
STD ERR OF EST -	6.13371
PLOTTED VALUES -	426
R SQUARED -	.43707
INTERCEPT (A) -	23.61255
EXCLUDED VALUES-	0
SIGNIFICANCE -	.00000
SLOPE (B) -	-.00622
MISSING VALUES -	0

GRADIENT OF TEMPERATURE: 0.622°C/100M

0°C-LINE AT 3796M

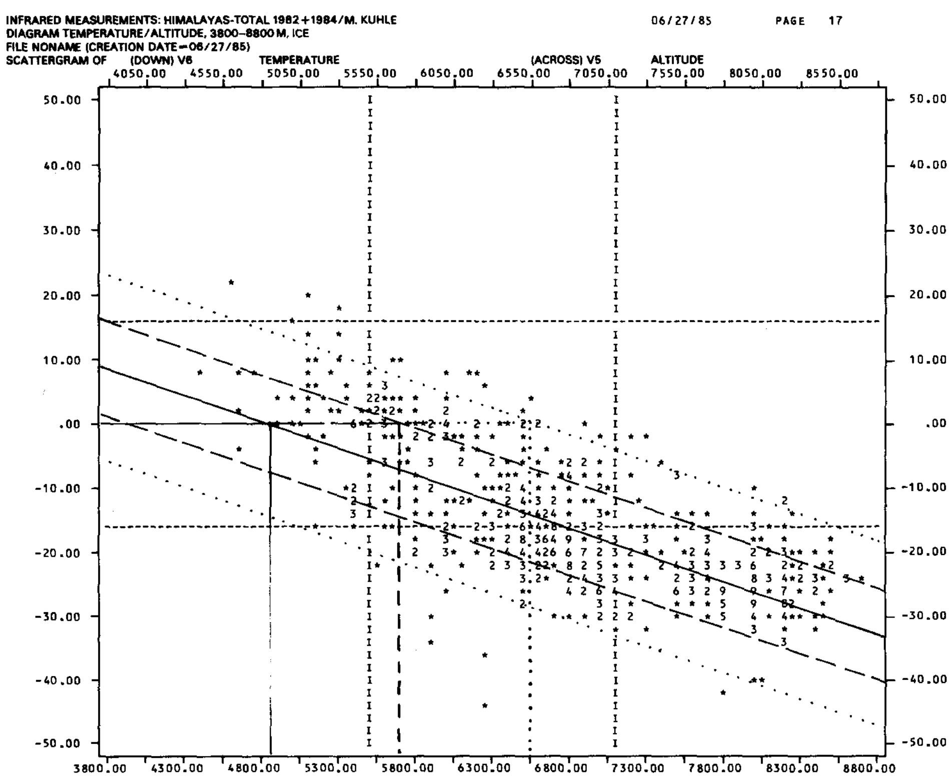

Fig 24

STATISTICS..

CORRELATION (R)-	-.73385
STD ERR OF EST -	7.29835
PLOTTED VALUES -	685
R SQUARED -	.53854
INTERCEPT (A) -	41.80658
EXCLUDED VALUES-	0
SIGNIFICANCE -	.00000
SLOPE (B) -	-.00851
MISSING VALUES -	0

GRADIENT OF TEMPERATURE: 0.851°C/100M

0°C-LINE AT 4913M

Fig 25

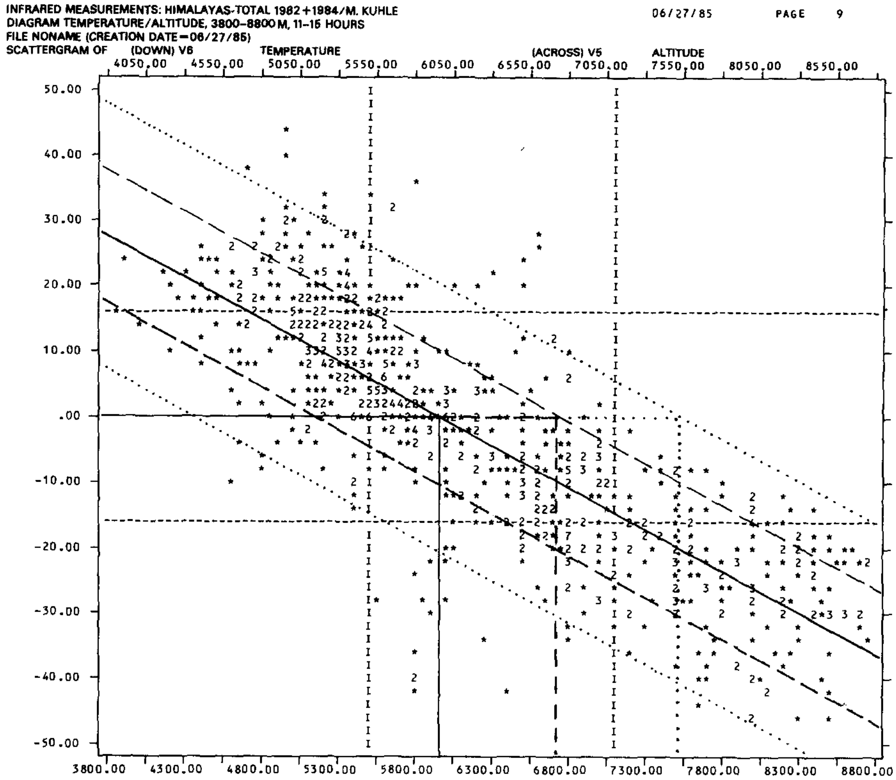

STATISTICS..

CORRELATION (R)-	-.82063
STD ERR OF EST -	10.23843
PLOTTED VALUES -	813
R SQUARED -	.67343
INTERCEPT (A) -	78.09186
EXCLUDED VALUES-	5
SIGNIFICANCE -	.00000
SLOPE (B) -	-.01309
MISSING VALUES -	0

GRADIENT OF TEMPERATURE: 1.309°C/100 M

0°C-LINE AT 5966 M

Fig 26

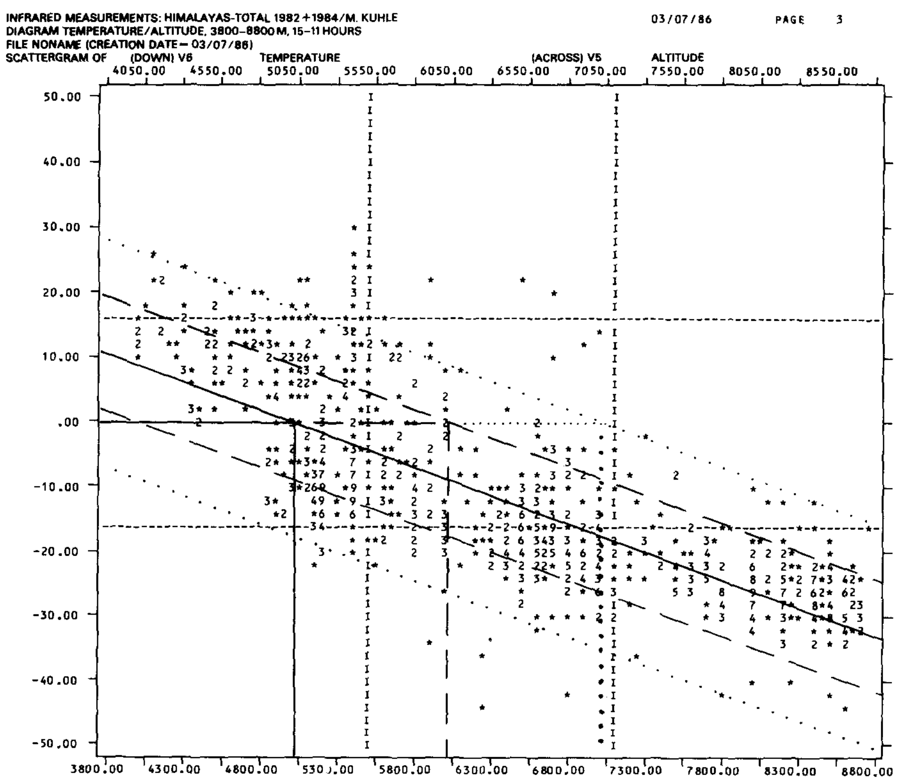

STATISTICS..

CORRELATION (R)-	-.78873
STD ERR OF EST -	8.86377
PLOTTED VALUES -	962
R SQUARED -	.62210
INTERCEPT (A) -	44.01068
EXCLUDED VALUES-	3
SIGNIFICANCE -	.00000
SLOPE (B) -	-.00878
MISSING VALUES -	0

GRADIENT OF TEMPERATURE: 0.878°C/100 M

0°C-LINE AT 5013 M

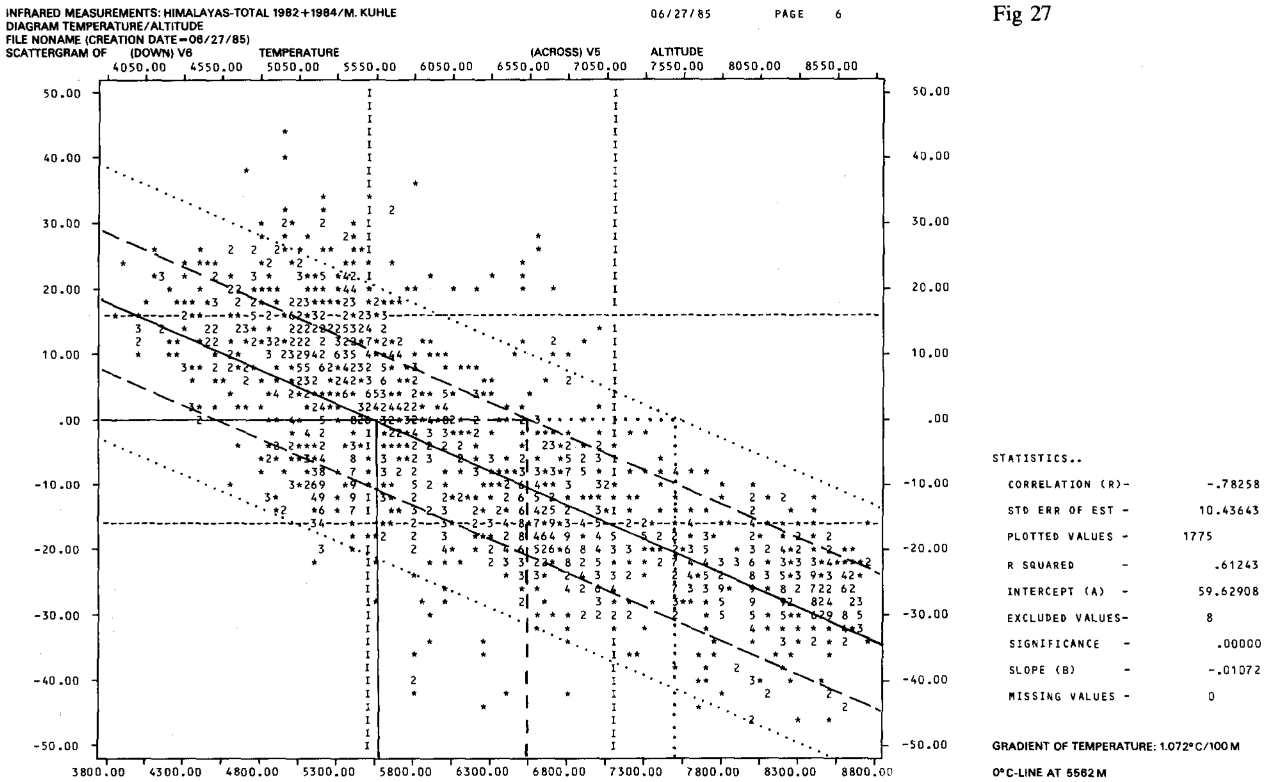

Fig 27

point. The daily average height of the 0° C line lies at 5719 m in contrast to 4913 m on surface of ice, firn and snow, i.e. a height difference of 806 m. This is also shown by the weakened temperature gradient over ice resulting from the loss of energy to latent heat during the melting process. The temperature gradient on rock surfaces is (according to time of day) between 0.23° C/ 100 m and 0.36° C/100 m greater than that on the ice surfaces; in the mean it is 0.2° C steeper (Fig 30).

The 7200 m upper glacial limit, which has been found by regression analysis and the application of single and double SEE values in the Mt. Everest, Makalu and Lhotse areas of the central Himalayas separates the zone of perennially snow-, firn- and ice-covered slopes from the seasonally snow-free rock (Fig 4, 5, 28, 29). Whereas by symmetry just as in the lower altitudinal zones of the High Himalayas as below the snow line (ELA) and far below the whole glacial region snow falls during winter remain lying; in the region above the upper glacial limit the snow falls in summer (during the monsoon precipitation; Fig 5 and 28). This does not melt like the snow at lower levels but is blown away during the winter. This region of glaciers is thus clearly bounded above and below. In the higher regions there are larger areas of rock and debris at the surface because the snow is blown away during the winter by the high velocity jet-stream (more than 45 m/sec) and prevented from compacting and adhering by the low temperatures. Only in areas of local lee eddies snow accumulations some decametres in thickness occur and pressure compaction of the cold snow into ice of density 830 kg/m^3 result. It is here that small hanging glaciers and ice ledges over 100 m thick form over several decades in such cold conditions, far above the real climatic upper glacial limit of 7200 m (Fig 4 /, 5 /). The age of such cornices may be determined by the large number of annual layers. Because of the extreme extra – zonal conditions, recognizable small glacial features are far apart and separated by snow-free rock slopes (Kuhle 1986b).

These rock and local debris surfaces (as extending on the N ridge of Mt. Everest from the N saddle (Fig 28) as well as on the 8000 m Mt. Everest S saddle) above the upper glacial limit belong to a *pergelid* (eternally frozen) rock and dry debris altitudinal zone. It is this zone, and not that of the glaciers, that is the highest planetary altitudinal zone. It is confined solely to the high peaks of the Himalayas, the Karakoram (Kuhle 1987a, photo 3) and to a few peaks in the Vinson massif (in the Antarctic at 80° S) above 3500–4000 m. During the pleistocene glaciation this zone was rather more extensive. At that time, because of the general reduction in temperature, the thermal upper glacial boundary must also have been lowered (see below). The zone of pergelid rock and dry debris is characterized by purely temperature weathering in a region of negative temperature. The coarse blocky debris found there can only be produced by a process of rock destruction independent of that of freezing and thawing. The bonds between crystalline components of

Fig 28 Summit pyramid of Mt. Everest from the East Rongbuk glacier at 6300 m seen from the N; to the right the main summit at 8874 m, to the left the rock towers of the East Ridge (8390 m). Although the N flanks of the mountain (especially below the main peak) (○) slope gently and stepwise (mean slope 36° to 43°), rock forms large areas of the surface and there is no ice on the walls and no hanging glacier formation. Perennial snow only collects in the stable lee locations of chimneys and couloirs (×). It is there converted to firn on the walls and ice on the flanks. The upper limit of glaciation occurs on the metamorphic rocks of the mountain between 7000 m and 7600 m where the rock is kept clear by the wind. Where measurements were made on the peak (○) mean temperatures of −28° C to −36° C were observed in autumn 1984 under radiation weather conditions.
Photo: M. Kuhle, 15 October 1984

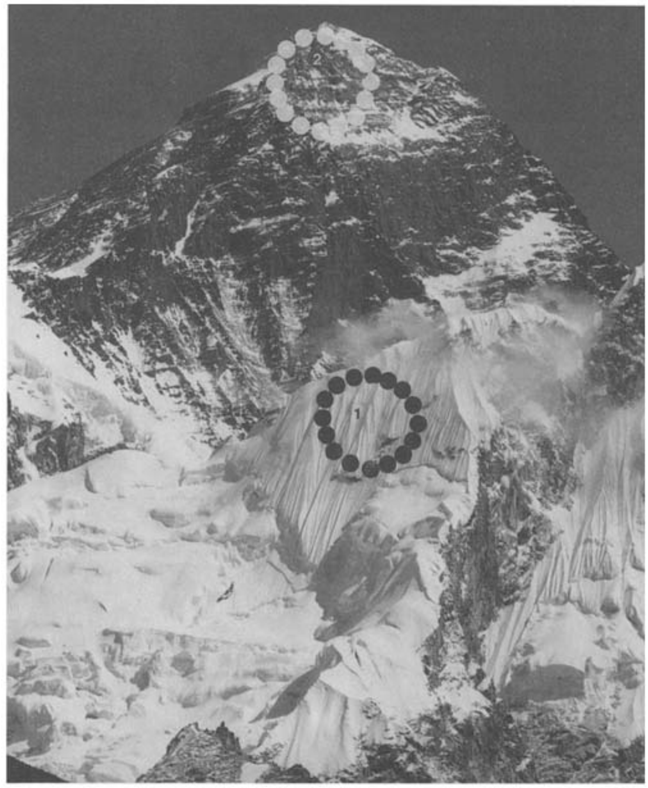

Fig 29 Mt. Everest viewed from the W at 5600 m. In the foreground the steep firn and glacier covered NW peak of Nuptse can be distinguished from the glaciated SSE slope of the WNW ridge of Mt. Everest. The locally only monsoon snow covered strata bands of the peak of Mt. Everest are not glaciated above 7000 to 7200 m. Under full sunshine conditions during 11 to 21 October 1982 measurements of surface temperatures on the firn between 6530 m and 6680 m (①) showed values of −7° C to 0° C but on rock between 8350 m and 8874 m (②) temperatures of −28° C to −46° C.
Photo: M. Kuhle, 19 October 1982

the rocks with different coefficients of expansion are destroyed by the temperature oscillations of 15° C to 25° C below the freezing point. Probably because of the reduced elasticity of the rock at lower temperatures the intensity of the weathering is greater than that of the insolation weathering in warm arid regions (e.g. the Sahara). Whilst on Earth this weathering is found only on a few high peaks it is of supra-regional significance on other planets. Thus for example the oscillations of surface temperature on Mars at the landing place of Viking I average −38° C to −85° C (Stanek 1980).

At the glacial maximum the snowline (ELA) depression in the area of investigation was 1200 m (Kuhle 1987b). In September and October the author used three stations between 3960 m and 5330 m in similar moisture conditions on the K2 glacier to measure gradients of air temperature of 0.7° C/100 m to calculate the cooling of the warmest month then of 8.4° C/100 m. In similar conditions Kuhn (1981; 1983) gave a lapse rate in the free air of 0.8° C/100 m which denotes a cooling of 9.6° C.

Since similar conditions of heat and mass balance apply to the thermal upper limit of glaciation and to the snowline (ELA) a comparable depression of 1200 m must have occurred. It cannot be excluded that such a depression of the upper limit of glaciation was a consequence of such steep gradients as 1.07 to 1.35° C/100 m (or even of 1.45 to 1.51° C/100 m according to Kuhle 1986a, Fig 1 and 2). It can thus be concluded that during the last glacial period there was a depression of the upper glacial limit of 620 to 1200 m to about 6000 m to 6580 m above present sea level. Thus on other less elevated mountain systems a pleistocene upper limit of glaciation must also be expected.

INFRARED MEASUREMENTS HIMALAYA 1982, 1984

material	time	0° C-line (a.s.l.)	temperature-gradient (° C/100 m)	number of values	altitudinal difference between 0° C-lines (m)	difference of temperature gradients (° C/100 m)
rock	11-15	6070	1.35	554	870	0.5
rock	15-11	5200	0.85	536		
rock	0-24	5719	1.05	1090	———	———
ice	11-15	5477	0.99	259	1681	0.37
ice	15-11	3796	0.62	426		
ice	0-24	4913	0.85	685	———	———
rock/ice	11-15	5966	1.31	813	953	0.43
rock/ice	15-11	5013	0.88	962		
rock/ice	0-24	5562	1.07	1775	———	———
rock	11-15	6070	1.35	554	593	0.36
ice	11-15	5477	0.99	259		
rock	15-11	5200	0.85	536	1404	0.23
ice	15-11	3796	0.62	426		
rock	0-24	5719	1.05	1090	806	0.2
ice	0-24	4913	0.85	685		

Draft: M. Kuhle

Fig 30
Table from the diagrams of Fig 19 to 27

Summary

1) Radiation measurements over a period of c. 2.5 months in S Tibet and on the Himalaya S slope up to heights of 6650 m showed very high values. These are close to the theoretical solar-constant values for corresponding solar altitudes. Measurements of radiation balance over snow surfaces of the glacier catchment areas show that up to 90% of this energy is reflected, whereas over debris surfaces this value ranges from 16 to 24%, about 70% lower than the former.

2) Observations and measurements of cloud cover, humidity, wind direction and velocity showed the transition from the summer monsoon to the radiation conditions of autumn and winter. This results from a change from variable low velocity winds to storm winds from the S to SE, and from humidities of up to 90% to those no more than 40 to 10%. Associated with the seasonal decrease in temperature is a freezing of the debris above 5000 m from September to November to a maximum depth of a few decimetres. Although the frost at the end of September penetrated only a few centimetres, by the beginning of November the diurnal thaw penetrated no deeper than 10 cm. Thus there were no more than 45 days of solifluction (periglacial) activity during this transitional season during which a 10–20 cm thick frost active layer moved downslope.

3) Data derived from telemetric measurements of surface temperatures between 3800 and 8800 m on debris, rock, ice, firn and snow on the slopes of the Himalayas were analysed statistically. The lapse rate of these temperatures was rather steeper than that of the free atmosphere, ranging from 0.85 to 1.35° C/100 m. Rock surfaces showed higher lapse rates (up to 1.35° C/100 m) than ice surfaces (up to 0.99° C/100 m). Simple and double SEE showed an absolute 0° C level on the Himalaya slopes at 7200 m. Average temperatures above this height are so low (less than −25° C) that, apart from sublimation and molecular diffusion, only very slow ice-bridge formation between the snow crystals can occur. Because high winds prevent the necessary persistence of snow cover (by deflation) there is at 7200 m an upper climatic limit to glacier formation. Above this level the highest altitudinal zone on Earth is formed of a pergelid rock and dry debris region. During the glacial period this empirical upper limit of glaciation was depressed parallel to the snowline (ELA) by between 620 m and 1200 m.

References

Bishop, C. B.; Ångström, A. K.; Drummond, A. J.; Roche, J. J.: Solar Radiation Measurements in the High Himalayas (Everest Region). Journal of Applied Meteorology, 5, 94–104 (1966)

Häckel, H.; Häckel, K.; Kraus, H.: Tagesgänge des Energiehaushalts der Erdoberfläche auf der Alp Chukhung im Gebiet des Mt. Everest. Khumbu Himal (zweite Lieferung), 47–60, München 1970.

Kuhle, M.: Permafrost and Periglacial Indicators on the Tibetan Plateau from the Himalaya Mountains in the south to the Quilian Shan in the north (28–40° N). Z. f. Geomorph. N. F. 29, 2, 183–192 (1985)

Kuhle, M.: Die Obergrenze der Gletscherhöhenstufe, Oberflächentemperatur und Vergletscherung der Himalayaflanken von 5000–8800 m. Z. f. Gletscherk. 22, 2, 149–162 (1986a)

Kuhle, M.: The Upper Limit of Glaciation in the Himalayas. GeoJournal 13, 4, 331–346 (1986b)

Kuhle, M.: Physisch-geographische Merkmale des Hochgebirges: Zur Ökologie von Höhenstufen und Höhengrenzen. Frankfurter Beiträge zur Didaktik der Geographie. 10, 15–40 Frankfurt am Main (1987a)

Kuhle, M.: Subtropical Mountain- and Highland-Glaciation as Ice Age Triggers' and the Waning of the Glacial Periods in the Pleistocene. GeoJournal 13, 6, 1–29 (1987b)

Kuhn, M.: Climate and Glaciers. Sea Level, Ice, and Climatic Change, Proceedings of the Canberra Symposium, Dec. 79, IAHS, 131, 3–20 (1981)

Kuhn, M.: Die Höhe der Schneegrenze in Tirol, berechnet aus Fliris klimatischen Profilen. Arbeiten zur Quartär- u. Klimaforschung. Innsbr. Geogr. Stud. 8, Fliri Festschrift, Innsbruck (1983)

Lorenz, D.: Die radiometrische Messung der Boden- und Wasseroberflächentemperatur und ihre Anwendung insbesondere auf dem Gebiet der Meterologie. Z. Geophys. 39, 627–701 (1973)

Shi Yafeng; Xie Zichu: The Basic Characteristics of the Existing Glaciers in China. Acta Geographia Sinica 30, 3, 1–38 (1964)

Stanek, B.: Planeten Lexikon. 3. Aufl., Hallwag, Bern, Stuttgart 1980.